Impact of Ionospheric Scintillation on Spaceborne SAR Observations Studied Using GNSS

Xiaoqing Pi[1], Franz J. Meyer[2], Kancham Chotoo[3], Anthony Freeman[1], Ronald G. Caton[4], and Christopher T. Bridgwood[5]

[1]*Jet Propulsion Laboratory, California Institute of Technology, Pasadena, CA*
[2]*Geophysical Institute, University of Alaska – Fairbanks, Fairbanks, AK*
[3]*User Systems, Inc., Crofton, MD*
[4]*Space Vehicles Directorate, Air Force Research Laboratory, Kirtland AFB, NM*
[5]*Boston College, Boston, MA*

BIOGRAPHIES

Xiaoqing Pi is a Senior Research Technologist at the Jet Propulsion Laboratory. He received B.S. degree in Radio Wave Propagation and Antenna and M.S. degree in Space Physics, both from Wuhan University, and Ph.D degree in Astronomy from Boston University. He has been working in the fields of ionospheric remote sensing and modeling for more than 20 years. He joined the Jet Propulsion Laboratory in 1996. Since then he has served NASA's, DoD's, and FAA's various science and technology programs and missions, and has received a number of NASA's Space Act Board awards and Certificates of Recognition. He has led a number of development projects at JPL including GPS scintillation monitoring system and network, software for Ionospheric Specifications for SAR Interferometry (ISSI), and Ionospheric Simulation System for Satellite Observations and Global Assimilative Model Experiments (ISOGAME). He is a co-inventor of Global Assimilative Ionospheric Model and the Rate of TEC Index for measuring ionospheric irregularities. Recently he has been a principal investigator of NASA's research projects for imaging the ionosphere using synthetic aperture radar and GPS, and for global mapping of ionospheric irregularities and scintillation using GNSS.

Franz J. Meyer received the Diploma in Geodetic Engineering and the Doctor of Engineering degree from Technische Universität München, Munich, Germany, in 2000 and 2004, respectively. Since 2008 he has been working for the University of Alaska Fairbanks where he currently is an Associate Professor for radar remote sensing. His interests include studies of ionospheric and tropospheric effects on SAR and InSAR, new methods of InSAR time series analysis, SAR Interferometry applications, SAR processing, and SAR data quality analysis. He has 12 years experience in radar data processing and is the author of more than 80 scientific publications, including four being acknowledged as "Best Papers". Dr. Meyer was the recipient of the IEEE Geoscience and Remote Sensing Society Gold Early Career Award 2011 for demonstrating outstanding ability and promise for significant contributions in the future.

Kancham Chotoo received his Ph.D in Physics from the University of Maryland in College Park and is currently a Senior Research Scientist and Vice President of User Systems, Inc. He has 20 years experience in data processing, calibration and analysis of space-based and airborne scientific instruments in the fields of space physics and synthetic aperture radar (SAR). Emphasis has been on SAR image formation processing, precision geolocation, exploitation and analysis of interferometric SAR imagery, coherent change detection, detection of ground moving targets (GMTI), exploitation and analysis of polarimetric imagery, and mitigation of ionospheric effects from SAR imagery.

Anthony Freeman received the B.Sc. (Hons.) degree in mathematics in 1979 and the Ph. D. degree in astrophysics in 1982, both from the University of Manchester Institute of Science and Technology, in his home town of Manchester, England. Dr. Freeman is currently the head of the Earth System Science Formulation Program at the Jet Propulsion Laboratory (JPL). Prior to this position, he was section manager of the Mission and Systems Architecture Section at JPL, responsible for all advanced mission studies at JPL and prior to that instrument manager for the LightSAR Radar Program at JPL. He has over 29 years of experience in radar systems. He is still active in research, and his

current interests include correction of Faraday rotation in radar propagation (including the Freeman method), modeling of polarimetric radar scattering signatures (including the Freeman-Durden Decomposition), and the design of innovative SAR systems and missions (e.g. the SweepSAR technique he developed for the DESDynI mission). Dr. Freeman is also an adjunct professor at the University of Southern California, teaching a graduate-level class on Remote Sensing Systems from Space. He teaches Systems Engineering for the California Institute of Technology. He has been awarded the NASA Exceptional Service Medal for calibration of SIR-C mission data, the NASA Exceptional Achievement Medal for his work on Earth Science Mission Formulation, several NASA Group Achievement Awards, numerous NASA new technology awards, and holds two patents. He was elected a Fellow of the IEEE in 2000.

Mr. Caton is a Research Physicist with the Space Vehicles Directorate of the Air Force Research Laboratory (AFRL). His primary area of interest is the equatorial ionosphere and the impacts of scintillation on navigation and communication systems. Mr. Caton joined AFRL in February 2009 after more than 13 years as a contractor with Radex Inc. and Atmospheric Environmental Research, Inc. working on various projects including the Scintillation Network Decision Aid (SCINDA). He has presented papers on his work at a variety of international assemblies including the Ionospheric Effects Symposium, the International Symposium on Equatorial Aeronomy, and meetings sponsored by the International Union of Radio Science. He has authored multiple Air Force Technical Reports and peer reviewed journal articles in *Radio Science*, *Geophysical Research Letters*, and the *Journal of Geophysical Research*. Mr. Caton received a Master's of Science degree in Physics from the University of Alabama in Huntsville in 1995 where he worked as a Research Assistant in the Center for Space Plasma, Aeronomy, and Astrophysics Research (CSPAAR). While a graduate student, he concentrated primarily on the dynamics of ionospheric upflows in the auroral region and published results from his research in *Geophysical Research Letters* and the *Journal of Geophysical Research*. Mr. Caton has been member of the American Geophysical Union since 1995.

Christopher Bridgwood is a Research Analyst with the Institute for Scientific Research at Boston College. He has 11 years experience in processing and analysis of space weather data recorded by AFRL SCINDA remote sensing instruments. He has performed science studies on ionospheric phenomenology that lead to co-authorship on several papers, including one that earned the Best Paper Award. He has B.S. and M.S. degrees in Applied Mathematics from the University of Massachusetts.

ABSTRACT

A survey of artifacts seen in JAXA's Phase Array type L-band synthetic aperture radar (PALSAR) data over South America during a low solar activity year is reported in this paper. A significant impact on the radar data is revealed: about 14% of the surveyed PALSAR images (totally 2779) are affected by the artifacts during a month and the artifacts occur on 74.2% of the surveyed days. The characteristics of the artifacts have led to a consideration that the artifacts are the effects of ionospheric scintillation. This raises not only a concern about scintillation effects on radar but also a question about active scintillation conditions during a low solar activity year. To assess and verify the scintillation conditions, GPS data collected from the constellation of FORMOSAT-3/COSMIC satellites and three ground-based GPS networks are processed and analyzed. The GPS data provides a global context and regional dense coverage, respectively, of ionospheric irregularity and scintillation measurements. It is concluded that even during a low solar activity year, L-band scintillation at low latitudes can occur frequently and affect L-band SAR significantly.

INTRODUCTION

L-band spaceborne radars have been increasingly applied to Earth science remote sensing satellite missions in recent years. The launched and planned L-band systems include JAXA's Phase Array type L-band Synthetic Aperture Radar (PALSAR) and its scheduled follow on, NASA's Aquarius, Soil Moisture Active and Passive (SMAP), and Deformation, Ecosystem Structure and Dynamics of Ice (DESDynI). The science objectives of these missions are to provide measurements such as sea surface salinity, soil moisture, surface deformation, vegetation, ice dynamics, etc., to study and monitor changes of land and sea as well as climate.

All these radar systems rely on L-band radio signals that traverse the ionosphere. Like GNSS systems, the L-band radar signals are also susceptible to ionospheric effects. The ionospheric effects on radio signals fundamentally include signal time delay, phase advance, Faraday rotation, and amplitude as well as phase scintillation. To the radar systems, the major concern about the ionospheric effects is possible artifacts and distortion in the Earth science images constructed based on the radar signals. For example, anomalous strips were found in PALSAR images over the Amazon region [1], and the feature was believed to be an effect of ionospheric scintillation. To interferometric synthetic aperture radar (InSAR) image constructions, ionospheric inhomogeneities of scales ranging from hundreds of meters to tens of kilometers along and cross the satellite path can also distort InSAR images [2, 3, 4, 5, 6, 7].

Identification and correction of ionospheric effects have become an important component in system design, data calibration, and image processing of the spaceborne L-band radar missions. The correction of ionospheric effects on radar imagery requires high-resolution measurements. This has led to the development of techniques to measure ionospheric effects using radar itself. Such a new capability has been demonstrated for high-resolution ionospheric imaging in different latitude regions, including ionospheric inhomogeneities associated with auroral arcs, mid-latitude trough, traveling ionospheric disturbances, and plasma bubbles as well as scintillation [5].

In this report, we will first present a survey of artifacts seen in PALSAR images over South America. As mentioned above, similar artifacts have been reported in previous studies [1]. The artifacts have also been recently simulated using ionospheric scintillation models [6, 7]. Here we provide GPS measurements of ionospheric irregularities and scintillation as independent evidence to verify the cause of the radar artifacts. Following a summary of the survey, we will examine ionospheric scintillation and irregularity measurements made in the regions of PALSAR paths using spaceborne and ground-based GPS receivers.

A SURVEY OF ARTIFACTS IN PALSAR DATA

PALSAR is one of the three major instruments carried by the JAXA's Advanced Land Observing Satellite (ALOS). The satellite was launched in January 2006, and decommissioned in April 2011. The satellite was flying in a sun-synchronous 10AM/10PM orbit at about 690 km altitude. During its five-year successful operation, ALOS has collected Earth image data covering 6.5 million scenes all over the world. The ALOS data has been used for disaster mitigation in regions damaged by earthquakes, tsunami, or typhoons, as well as for forest monitoring, natural environment maintenance, agriculture, and topographical map.

The L-band (1.27 GHz) PALSAR operated in several modes including ScanSAR, fine resolution, and polarimetric mode. During the five years, the radar data collected along ascending orbit paths (10 PM) often show distinguished artifacts in low-latitude images. Figure 1 shows such an ascending path in the South America region and the ground locations of 10 image frames along the path at about 03:19 UT on October 31, 2010. Examining these images, we have found that all 10 images show artifacts, i.e., features of streaks, in the intensity of the images. Figure 2 presents two examples (the 6th and 7th image from bottom) from the 10 images. A couple of features are noticed besides image blurring as the streaks are present: (1) the streaks are aligned with the ambient geomagnetic field, the latter's orientation marked by a red line in each image; (2) the streaks appear in fine-resolution (kilometer to sub-kilometer) structures quasi-periodically in the direction perpendicular to the magnetic field line.

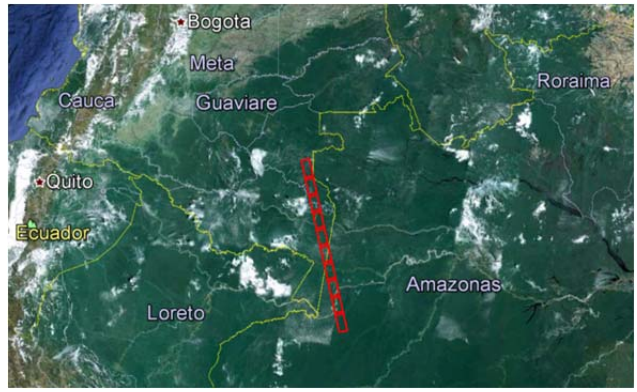

Figure 1. Locations of 10 PALSAR image frames along an ALOS ascending orbit path over South America on October 31, 2010.

To investigate the phenomenon statistically, we have conducted a survey of the streak artifacts seen in PALSAR images. In this survey we examined totally 2779 PALSAR images collected over South America during October 2010. A summary of the survey is shown in Figure 3. We have found through this survey that 14% of PALSAR images are contaminated by the streaks, and the contaminated images appear on 74.2% of the days in the month. The survey result brings an alarm: (1) the effects are quite significant and must be dealt with; (2) the cause of the effects must be identified.

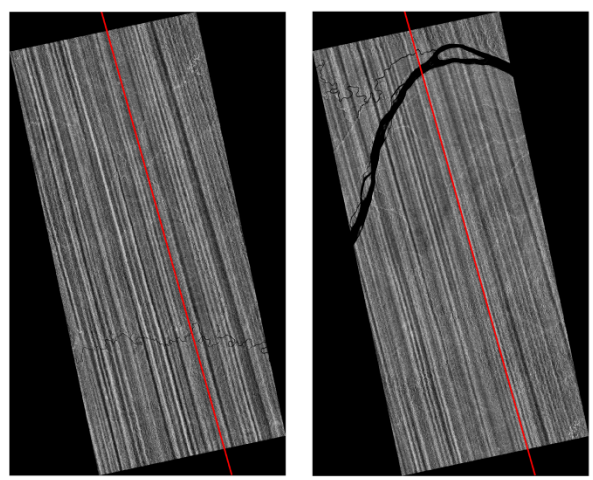

Figure 2. Two examples of the PALSAR images collected over a South America low-latitude region (referring to Figure 1, near 2°S, 290°E) at about 03:19 UT on October 31, 2010. The red lines overlapped on the radar images indicate the orientation of the ambient geomagnetic field projected from 350 km altitude. The images show streak features that are aligned with the ambient geomagnetic field.

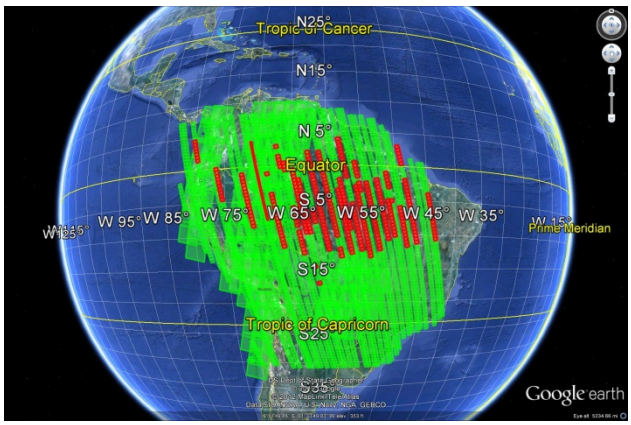

Figure 3. A summary plot showing the surveyed PALSAR images collected from South America during October 2010. The green color marks uncontaminated images while the red color indicates the images showing streaks as shown in Figure 2. It is found in this survey that 14% of PALSAR images are contaminated by the streak artifacts during October 2010, and the contaminated images appear on 74% of the days in the month.

The following unique features of the streaks have led us to consider that the effects are due to ionospheric scintillation:

(1) the streaks are aligned with the ambient geomagnetic field, which is consistent with our knowledge of ionospheric irregularities that tend to elongate along the magnetic field;

(2) the streaks occur during a high season of ionospheric scintillation season in the region;

The magnetic alignment of ionospheric irregularities and associated radar streak features have been investigated in a recent simulation studies [6, 7], which apply phase screen models and anisotropic properties to the simulated irregularities. The simulations were able to reproduce the SAR streaks using the irregularity model.

However, we also notice that surveyed PLSAR data was collected in a low solar activity year. Figure 4 plots the 10.7 cm solar radio flux index and the planetary magnetic Ap index data for September, October, and November of 2010 (in blue). As a comparison, the same indices 11 years ago during the last solar cycle are also provided in the figure (in red). Both solar and magnetic data indicate near solar minimum conditions when F10.7 index was around 80's and Ap rarely reached 20 during the October (Ap ≥ 25 or 30 indicates disturbed space weather and magnetic conditions). It has been acknowledged based on decades of studies that ionospheric scintillation wouldn't be so active during low solar activity years. The high occurrence of SAR artifacts seems contradicting our knowledge. In addition, the periodic streaks in the direction perpendicular to the ambient geomagnetic field have not been observed by other instruments in the past including ground-based all-sky cameras and incoherent scatter radars. Whether the fine structures (kilometer to sub-kilometer) in streaks are due to radar's high-resolution capability or they are real irregularity features are a puzzle.

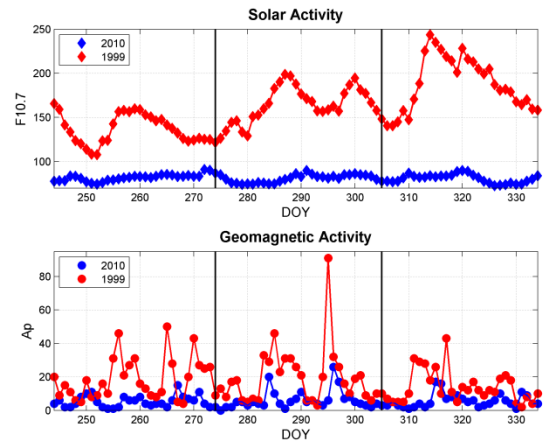

Figure 4. The 10.7 cm solar radio flux index and planetary magnetic Ap index during September, October, and November of 1999 (red) and 2010 (blue).

Ionospheric Scintillation Measured Using GPS Radio Occultation Receivers onboard COSMIC Satellites

To assess the high occurrence of the streaks seen in L-band PALSAR data, we turn to GPS data. First we processed amplitude scintillation data collected using GPS radio occultation (RO) receivers onboard the constellation of 6 FORMOSAT-3/COSMIC low Earth orbiters (~800 km altitude). COSMIC (Constellation Observing System for Meteorology, Ionosphere and Climate) is a joint Taiwan and the U.S. satellite mission. The GPS RO receivers carried by the COSMIC satellites were designed by JPL and manufactured by the Broad Reach Engineering. The original receivers did not include ionospheric scintillation measurements in the receiver design. This capability was incorporated in a software update by JPL after the mission was launched. Due to the limitation of the original system design, the upgraded capability only includes a measurement of amplitude scintillation S_4 index proxy. The algorithm of the proxy was jointly developed by UCAR and JPL, i.e.,

$$S_4 = \frac{\sqrt{\langle (I - \overline{\langle I \rangle})^2 \rangle}}{\overline{\langle I \rangle}}$$

where

$$I = SNR^2 ,$$

$$\langle I \rangle = \sqrt{\frac{1}{2}\sigma_I^2 + \langle SNR \rangle^4},$$

$$\sigma_I = \sqrt{\langle (I - \langle I \rangle)^2 \rangle},$$

and *SNR* is L1-C/A signal to noise ratio sampled at 50 Hz, $\langle I \rangle$ is 1-second averaged intensity approximately, $\overline{\langle I \rangle}$ is the low-pass filtered intensity average, and S_4 is measured for 1-second intervals.

Figure 5 shows an example of S_4 proxy (briefly S_4 hereafter) profile along with an electron density profile obtained from data collected on October 1, 2009, using a GPS RO receiver onboard the COSMIC-4 satellite tracking the GPS PRN19 satellite. Both data types are sampled at 1 second intervals, and the density profile is derived using an Abel inversion technique. The profiles use the altitudes of RO tracking tangent points (TP's, the points closest to the center of the Earth from the radio path at different epochs). The labeled local times ~20:17:23 and 20:17:31 correspond to the times of the maximum electron density and maximum S_4, respectively at the TP geographic locations (~4.086°S, 37.336°E). It is noticed that scintillation measured using the spaceborne receiver shows activity in E region (~110 km) and F region (above ~150 km). Through examining a large amount S_4 profiles, we have found that scintillation could be categorized into two types: E- and F-region scintillation. The E-region scintillation can be largely attributed to the layering change that occurs in a narrow altitude range, while the F-region scintillation can be attributed to F-region plasma irregularities that often range several hundreds of kilometers. We believe that F-region irregularities may more likely cause the artifacts seen in the L-band radar data. This is because the radar signals traverses through a much large range of irregularities in the F region than in the E region.

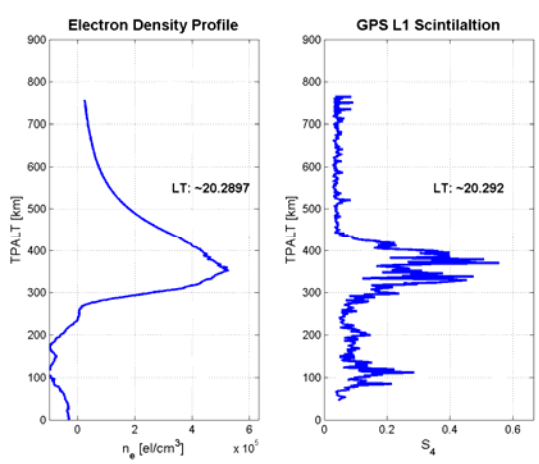

Figure 5. Electron density and scintillation S_4 profiles obtained on October 1, 2009, using a GPS radio occultation receiver onboard the COSMIC-4 satellite.

Based on the above assessment, we binned S_4 data measured in each 5° × 15° region (latitude × longitude) through the entire globe and in the range of 150 km to 600 km TP altitudes, using data collected from all 6 COSMIC satellites in the entire October 2010. In addition, the scintillation data is also binned in 5° × 1 hour region (latitude × local time). With such binned data, we computed scintillation occurrence rate. The rate is defined as the number of $S_{4,max} \geq 0.3$ events divided by the total number of S_4 profiles in each bin, where $S_{4,max}$ is the maximum S_4 in a profile. The occurrence rate is shown in Figures 6 and 7 for latitude vs. longitude and latitude vs. local time, respectively.

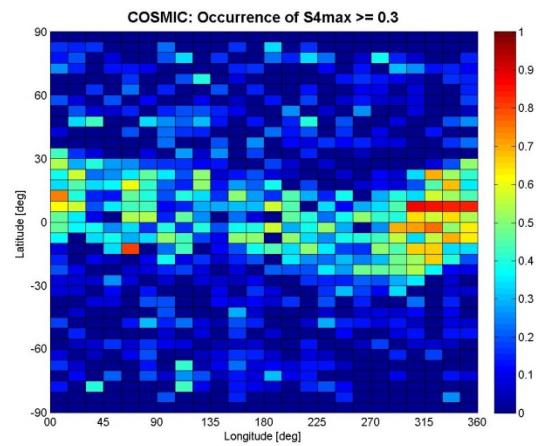

Figure 6. Scintillation occurrence rate as a function of longitude and latitude derived from COSMIC GPS observations made during October 2010.

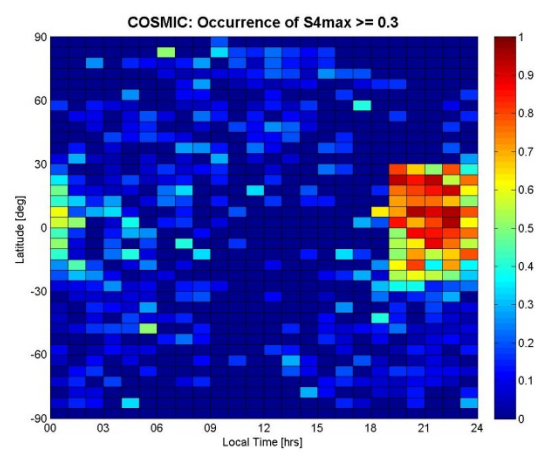

Figure 7. Scintillation occurrence rate as a function of local time and latitude derived from COSMIC GPS observations made during October 2010.

The occurrence rate derived from the COSMIC data shows similar scintillation patterns derived from ground-based measurements in the past. These patterns include:

(1) Most of L-band amplitude scintillation occurs at low latitudes, and the curved latitude zone of scintillation follows the offset between geomagnetic and geographic latitudes. For example, the largest offset is about -11 degrees near 290°E and about 11 degrees near 0°E (the Greenwich meridian).

(2) L-band amplitude scintillation rarely occurs at middle and high latitudes. We emphasize that although L-band amplitude scintillation does not often occur at high latitudes (including auroal zone and polar cap), phase scintillation does occur particularly under disturbed space weather conditions. We will not further discuss the polar scintillation here since it is out of the scope of this paper.
(3) The low-latitude amplitude scintillation mostly occurs during evening hours and some activity is also seen in post-midnight hours.

These patterns are consistent with past ground-based measurements, but the spaceborne data also covers the regions less accessible to ground instruments such as oceans. This makes a real global coverage possible and fills the gaps of ground-based measurements.

We notice that total counts of COSMIC GPS observations in the longitude × latitude and local time × latitude bins of PALSAR observations are about 10~25 and 10~30, respectively. Although the samples of measurements in each regional bin are limited, the high occurrence of scintillation measured by the COSMIC constellation shows consistency with that of radar artifacts over South America.

Ionospheric Irregularities Measured Using Ground-Based GPS Networks

Although the data collected from the COSMIC constellation provides a global context of scintillation activity for the concerned month of a low solar activity year, its regional data sampling in a short interval is very coarse. To investigate individual PALSAR events in details, we turn to measurements made using ground-based GPS receivers of three networks in South America: International GNSS Service (IGS), Low-latitude Ionospheric Sensor Network (LISN) [8], and Scintillation Network Decision Aid (SINDA) [9].

Although the receivers from these three networks all track GPS signals, the data recorded are of different types. The standard IGS data includes dual-frequency carrier phase and code pseudorange at 30-second cadence besides GPS satellite ephemeris. LISN is equipped with specialized scintillation receivers, and it records amplitude scintillation S_4 at 1-minute cadence and standard GPS phase as well as code range data at 30-second cadence. SCINDA is also equipped with specialized scintillation receivers, and it collects S_4 and TEC data at 1-minute cadence. To compare radar artifacts and GPS-based ionospheric irregularity/scintillation measurements seen at same locations at same time, we intend to maximize the spatial coverage density in the regions of PALSAR paths. This drives us to use the rate of TEC index (ROTI) measurements [10] that can be derived from GNSS dual-frequency phase data. Briefly, ROTI is defined as

$$\mathrm{ROTI} = \sqrt{\langle(\mathrm{ROT} - \langle\mathrm{ROT}\rangle)^2\rangle}, \quad \text{(TECU/minute)}$$

where ROT is detrended rate of line-of-sight TEC change, and ROTI is at 5-minute cadence. One advantage of using ROTI is to map densely distributed measurements to ionospheric piercing points (IPP), which provides ROTI map of snapshot of ionospheric irregularities. An example of such global ROTI maps for a space weather event on March 9, 2012, is given in Figure 8. We would like to mention here that ROTI and S_4 measurements are correlated at low latitudes based on studies of low-latitude ionospheric irregularities and scintillation [11].

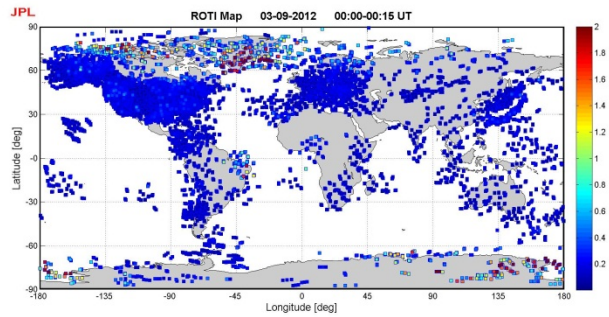

Figure 8. An example of global ROTI map produced at JPL using GPS data for a global snapshot of ionospheric irregularities.

For this study, we compare ROTI data with the PALSAR data described in the radar data survey section (Figures 1 and 2). Within a latitudinally bounded South America region as shown in Figure 8, GPS dual-frequency data from 12 IGS stations and 14 LISN stations accessible online are processed to produce ROTI measurements. Scintillation S_4 data from 5 SCINDA stations are also analyzed to identify the days when scintillation and artifacts are seen or not in GPS and PALSAR data.

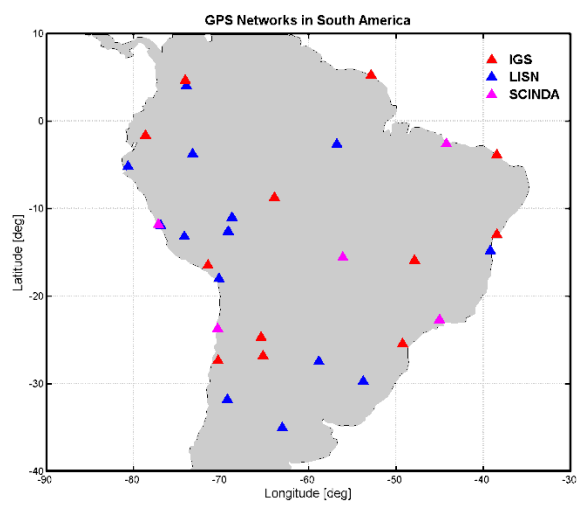

Figure 8. Distribution of IGS, LISN (partial), and SCINDA networks in South America.

Using the GPS data, we generated South America regional ROTI maps for every 15-minute intervals of October 31, 2010. Examining the ROTI maps, we have found increased ROTI surrounding the ALOS path before, during and after the time of satellite flyby at about 03:19 UT. Figure 9 presents a snapshot of ROTI regional map for the 03:15 – 03:30 UT interval. To provide a non-scintillation contrast, we also include Figure 10, which shows ROTI map at 12:15 – 12:30 UT when there is no scintillation activity in the region.

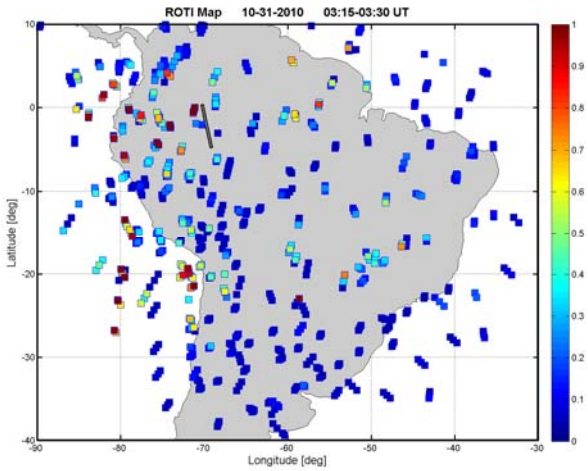

Figure 9. A snapshot of ROTI regional map for the 03:15 – 03:30 UT interval. ROTI values are color-coded in TECU/min. A narrow strip (near ~2°S, -70°W) represents the ALOS path at about 03:19 UT on October 31, 2010. Increased ROTI values indicate irregularity/scintillation activities in South America when ALOS flew by.

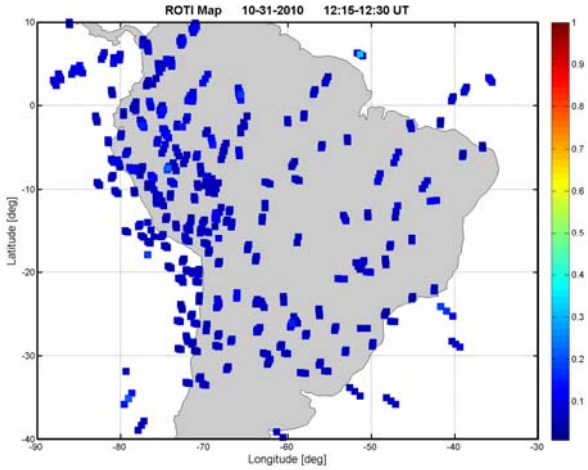

Figure 10. A snapshot of ROTI regional map for the 12:15 – 12:30 UT interval, indicating non-scintillation conditions in South America. ROTI values are color-coded in TECU/min.

In addition, ROTI measurements by individual receivers are also examined to find the correspondence of the location and time of the radar artifacts and ionospheric irregularities/scintillation. Figure 11 shows time sequences of ROTI and ROT measurements made along the radio links of receivers-to-GPS58 (space vehicle number) from Bogota (Colombia) and Riobamba (Ecuador). Relative line-of-sight TEC, elevation angles of observations, and tracking trajectories of IPP's at 400 km are also included in the plots. The detailed examinations confirm the activity of ionospheric irregularities during PALSAR observations in the region.

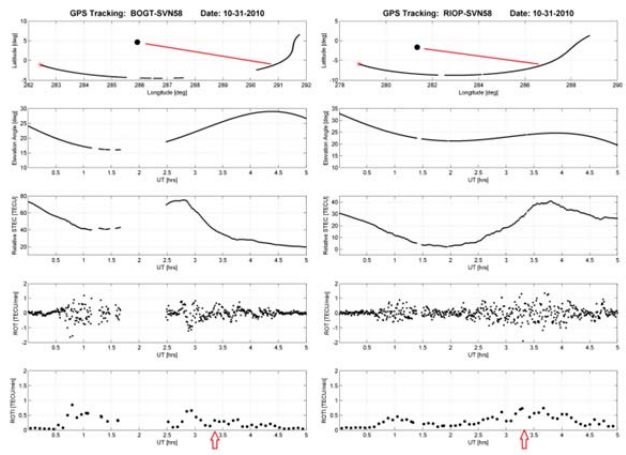

Figure 11. ROTI and ROT along with relative line-of-sight TEC measured by IGS GPS receivers at Bogota (Colombia) and Riobamba (Ecuador). In the top panels, the solid circles indicate observing sites, the red stars indicate the observation starting points of the plots, and the red lines from the stations point to approximately the IPP locations near the ALOS path (~2°S, 290°E) at about 03:19 UT (marked by red arrows on the bottom of the plots).

Conclusions

A survey of artifacts seen in PALSAR data has been performed with 2779 images collected over South America during October 2010. About 14% of the images show distinguished artifacts, i.e., streaks, and the streaks occur on 74.2% of the surveyed days during the month. The streaks are aligned with the ambient geomagnetic field and show quasi-periodic intensity features in the direction perpendicular to the geomagnetic field. The intensity of and the distance between the streaks in each image are random, and the distance ranges from sub-kilometers to 1 or a few kilometers. The characteristics of the artifacts indicate that the effects are likely due to ionospheric scintillation.

GPS L1 amplitude scintillation data (S_4) and ROTI data collected from the 6 COSMIC satellites and three ground-

based networks are processed and analyzed to compare with the characteristics of PALSAR artifacts. The spaceborne GPS scintillation measurements provide a global context of ionospheric scintillation for the concerned month, and ground-based GPS ROTI measurements provide a dense regional coverage of ionospheric irregularity observations. The GPS data conforms that even during a low solar activity year, L-band scintillation at low latitudes can occur frequently and affect L-band SAR significantly.

ACKNOWLEDGMENTS

The research at Jet Propulsion Laboratory, California Institute of Technology, is conducted under a contract with the National Aeronautics and Space Administration. The GPS scintillation analysis has been partially supported by the Federal Aviation Administration. and The authors are also grateful to Japanese Aerospace Exploration Agency and the Earth Observation Research Center (Japan), the International GNSS Service, Alaska Satellite Facility, Space Vehicles Directorate of the Air Force Research Laboratory (Kirtland, NM), and Cesar Valladares from Boston College for making PALSAR, GNSS, and GPS scintillation data available to this study.

REFERENCES

[1] Shimada, M., Y. Muraki, and Y. Otsuka (2008), Discovery of anomalous stripes over the Amazon by the PALSAR onboard ALOS satellite, IEEE International Geoscience and Remote Sensing Symposium, Boston, MA.

[2] Meyer, F., and J. Nicoll (2008), Ionospheric effects on SAR, InSAR, and SAR polarimetry—Theory and experiences with ALOS/PALSAR, paper presented at the 2008 IEEE International Geoscience and Remote Sensing Symposium, Inst. of Electr. and Electron. Eng., Boston, MA.

[3] Freeman, A., X. Pi, B. Chapman, and E. Chapin (2008), Evaluation of GPS vs. polarimetric based approaches for correction of Faraday rotation in SAR data, paper presented at the 2008 IEEE International Geoscience and Remote Sensing Symposium, Inst. of Electr. and Electron. Eng., Boston, MA.

[4] Rosen, P., E. Chapin, C. Chen, and S. Hensley, (2009), Ionosphere effects in polarimetric and interferometric SAR imagery, IEEE International Geoscience and Remote Sensing Symposium, Cape Town, South Africa.

[5] Pi, X., A. Freeman, B. Chapman, P. Rosen, and Z. Li (2011), Imaging ionospheric inhomogeneities using spaceborne synthetic aperture radar, J. Geophys. Res., 116, A04303, doi:10.1029/2010JA016267.

[6] Carrano, C. S., K. M. Groves, and R. G. Caton (2012), Simulating the impacts of ionospheric scintillation on L band SAR image formation, Radio Sci., 47, RS0L20, doi:10.1029/2011RS004956.

[7] Roth, A.P., B.D. Huxtable, K. Chotoo, S.D. Chotoo, R.G. Caton (2012), Detection and mitigation of ionospheric stripes in PALSAR data, IGARSS Proceedings, Munich, Germany, July, 2012.

[8] Valladares, Cesar E., Doherty, Patricia H. (2009), The Low-Latitude Ionosphere Sensor Network (LISN), Proc. of the 2009 International Technical Meeting of The Institute of Navigation, pp. 16-24, Anaheim, CA, January 2009.

[9] Groves, K. M., et al. (1997), Equatorial scintillation and systems support, Radio Sci., 32, 2047–2064, doi:10.1029/97RS00836.

[10] Pi, X., A. J. Mannucci, U. J. Lindqwister, and C. M. Ho (1997), Monitoring of global ionospheric irregularities using the worldwide GPS network, *Geophys. Res. Lett*., *24*, 2283, 1997.

[11] Beach, T. L., and P. M. Kintner (1999), Simultaneous Global Positioning System observations of equatorial scintillations and total electron content fluctuations, J. Geophys. Res., Vol. 104, no. a10, pages 22,553-22,565, October 1, 1999.